



HAL
open science

Non - electrochemical Na – deintercalation from O₃ NaVO₂

Daria Iermakova, Patrick Rozier, Jean-Yves Chane-Ching, Pierre-Louis Taberna, Patrice Simon

► **To cite this version:**

Daria Iermakova, Patrick Rozier, Jean-Yves Chane-Ching, Pierre-Louis Taberna, Patrice Simon. Non - electrochemical Na – deintercalation from O₃ NaVO₂. *Materials Research Bulletin*, 2020, 121, pp.110586. 10.1016/j.materresbull.2019.110586 . hal-02521034

HAL Id: hal-02521034

<https://hal.science/hal-02521034>

Submitted on 27 Mar 2020

HAL is a multi-disciplinary open access archive for the deposit and dissemination of scientific research documents, whether they are published or not. The documents may come from teaching and research institutions in France or abroad, or from public or private research centers.

L'archive ouverte pluridisciplinaire **HAL**, est destinée au dépôt et à la diffusion de documents scientifiques de niveau recherche, publiés ou non, émanant des établissements d'enseignement et de recherche français ou étrangers, des laboratoires publics ou privés.



Open Archive Toulouse Archive Ouverte (OATAO)

OATAO is an open access repository that collects the work of Toulouse researchers and makes it freely available over the web where possible

This is an author's version published in: <http://oatao.univ-toulouse.fr/25600>

Official URL: <https://doi.org/10.1016/j.materresbull.2019.110586>

To cite this version:

Iermakova, Daria and Rozier, Patrick^{ORCID} and Chane-Ching, Jean-Yves^{ORCID} and Taberna, Pierre-Louis^{ORCID} and Simon, Patrice^{ORCID} *Non - electrochemical Na – deintercalation from O₃ NaVO₂*. (2020) *Materials Research Bulletin*, 121. 110586. ISSN 0025-5408

Any correspondence concerning this service should be sent to the repository administrator: tech-oatao@listes-diff.inp-toulouse.fr

Non - electrochemical Na – deintercalation from O3 NaVO₂

Daria Iermakova^{a,b}, Patrick Rozier^a, Jean-Yves Chane-Ching^a, Pierre-Louis Taberna^{a,b},
Patrice Simon^{a,b,*}

^a Université Toulouse III- Paul Sabatier, CIRIMAT UMR CNRS 5085, 118 route de Narbonne, 31062 Toulouse Cedex 9, France

^b Réseau Le Stockage Electrochimique de l'Energie (RS2E), FR CNRS 3459, France

ARTICLE INFO

Keywords:

NaVO₂
Liquid exfoliation
Layered oxide
Sodium deintercalation

ABSTRACT

Layered oxides have been intensively studied for decades for their characteristics as electrode materials or their physical properties resulting from their structure. In this work, we present a modification of layered oxide NaVO₂ via liquid exfoliation technique in water. This oxide has VO_x layers with Na ions trapped in between. The goal of this process is to initiate sodium removal from the lattice, which will result in the structural transformations. During this sodium deintercalation, we observed drastic changes in the structure and electrochemical behavior of the oxide. Following water treatment, NaVO₂ exhibited nearly linear slopping discharge voltage profile and none of the multi-step reaction potential plateaus were observed, contrary to the profile of the pristine powder. Interestingly, this material structure was able to cycled reversibly within a much larger voltage window, with decent capacity value (ca 160 mAh/g), compare to pristine NaVO₂. Thanks to this change of behavior, the active material mean operating voltage was increased.

1. Introduction

Electrochemical energy storage had captured interest of the scientific community for decades due to its broad range of applications from cell phones to electric power grids. A lot of efforts have already been put in the development of high energy density devices such as lithium ion batteries, which achieve today the best performance (240 Wh.kg⁻¹), sodium ion batteries (SIB) etc. However, most of these devices fails so far to keep high power performance together with high energy density delivery. In order to meet the growing energy demands for energy storage systems, it is necessary to increase the power density of the device without sacrificing its energy density and cycle life.

Alternatively, capacitive energy storage offers some new interesting properties such as high power, long cycle life and fast charging mechanism. Electrochemical capacitors (ECs), also known as super capacitors, are capable of delivering / harvesting higher power (> 10 kW.kg⁻¹) and long cycle life compare to batteries, though energy performance is still a big issue (about 10 Wh.kg⁻¹). ECs could be roughly divided into two major groups, depending on the charge storage mechanism: Electrical Double Layer Capacitors (EDLCs) store the charge electrostatically in the electrochemical double layer formed at high surface area carbons from charge separation at the carbon / electrolyte interface [1]. Differently, charge storage mechanism in pseudocapacitive materials come from electron charge transfer.

Pseudocapacitance is then not electrostatic in origin; it is a surface confined redox reaction, which is not limited by solid state diffusion unlike faradic storage in battery type materials, which involved redox reactions in the bulk of the materials [2]. Since these materials use fast redox reactions, they held great promise for improving energy densities compared to EDLCs [3]. There is a variety of different classes of pseudocapacitive materials, and the most common ones are the transition metal oxides (RuO₂, MnO₂, Fe₂O₃, Nb₂O₅ etc) [4,5]. These materials can be used in asymmetric cells, where pseudocapacitive transition metal oxide electrode is combined with EDLC carbon material [6]. The resulting capacitance improvement almost twice of that of symmetric EDLCs combined with higher cell voltage make these materials very promising for preparing the next generation of high energy hybrid supercapacitors. However, pseudocapacitive transition metal oxides do have few major flaws like low electronic conductivity, low stability and difficulty maintaining high rate capability.

Considering the fact that in such aforementioned electrochemical redox reaction, in most of the cases, occurs at the surface (or near surface) of the material grains and not in the bulk it appears appealing to increase reactive surface as much as possible. This is even more true, since transport of ions of the electrolyte to all active sites continue to be a determining kinetic step; besides, another disadvantage of pseudocapacitive materials, especially oxides, is low electronic conductivity [7]. One of the approaches proposed in the

* Corresponding author at: Université Toulouse III- Paul Sabatier, CIRIMAT UMR CNRS 5085, 118 route de Narbonne, 31062 Toulouse Cedex 9, France.

E-mail address: simon@chimie.ups-tlse.fr (P. Simon).

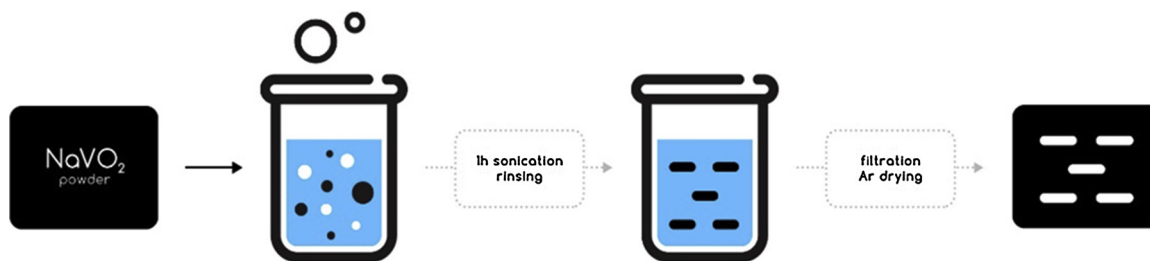


Fig. 1. Schematic representation of the NaVO₂ delamination process where water used as an oxidizer.

literature to tackle those issues is to design materials with tailored and controlled structures, such as the preparation of two dimensional (2D) materials by exfoliating materials into few layered or monolayered nanosheets [8].

Numerous studies have been already done on the liquid exfoliation of various compounds [9–12], that enables the formation of thin films and is potentially scalable [10]. This can be achieved by oxidation, ion intercalation/exchange, or surface passivation by solvents [9].

Much effort has been devoted to liquid exfoliation of graphene [13–15], though it has also been shown for some other materials, such as layered oxides [16], transition metal dichalcogenides [17] or metal carbides (MXenes) [18]. The latter has proved to be an excellent pseudocapacitive two dimensional material for different applications, from aqueous systems to hybrid Na ion supercapacitors [19,20]. Na_xVO₂ is a lamellar compound built with [VO₂]⁻ and Na⁺ layers. NaVO₂ synthesis was reported for more than 30 years ago by Barker et al. [21] then by Chamberland et al. [22]. After a long break, NaVO₂ synthesis was revisited by Onoda, who show the possibility to generate, depending on the sodium content, two types of lamellar compounds namely O3 NaVO₂ [23] and P2 Na_{0.70}VO₂ phase. These compounds differ by the stacking sequence of [VO₂] layers leading to define octahedral (O type) or prismatic (P type) sites for sodium while the number 3 or 2 corresponds to the number of [VO₂] layers in the unit cell. Then, Hamani et al. as well as Delmas et al. reported successful synthesis of various polymorphs of Na_xVO₂ via solid state and electrochemical deintercalation methods, with amount of Na varying from x = 0.5–1 [24–28]. It was also reported that NaVO₂ does not exhibit superior electrochemical properties, such as 120 mA h/g capacity and a mean operating voltage of 1.9 V (from 1.2 to 2.5 of voltage range), making such compound less appealing although some authors reported that it could be of interest after deintercalation [24].

This study focuses on the structure modification of NaVO₂ for pseudocapacitive storage applications. Owing the fact that NaVO₂ has VO₂ layers with Na ions trapped in between and that Na ions could be easily removed during electrochemical cycling [26] as well as during exposure to air (moisture) [27], it is tempting to try to remove more Na from the structure and target the achievement of delaminated pure VO₂ individual layers using a simple method based on liquid exfoliation technique, using the most abundant solvent existing water.

2. Experimental part

O3 type NaVO₂ was prepared by NaVO₃ reduction under H₂ at atmosphere, first at 500 then at 700 °C in a tubular furnace for 2 and 4 h respectively. NaVO₃ was synthesized via solid state reaction of Na₂CO₃ (Aldrich) and V₂O₅ under air at 520 °C for 12 h. The obtained powder was immediately transferred into the argon filled glow box with minimum exposure to air.

The delamination of the sample consisted in immersion of NaVO₂ powder in water, sonication of the solution for 1 h and filtration. This procedure was repeated multiple times until reaching neutral pH value of the solution. Collected powder was dried using lyophilization technique (freeze drying) or under Ar at 200 °C during 24 h.

The morphology of the obtained samples was characterized by

scanning electron microscopy, using JSM 6510LV Scanning Electron Microscope, and crystal structure by X ray powder diffraction measurement using a Bruker D4 diffractometer (CuKα radiation) in a 2θ range from 10° to 60° with 2θ angle step of 0.016°.

Electrodes were prepared by mixing 85 wt% of active material (pristine or treated NaVO₂) with 15 wt% of acetylene black then dried at 120° for 12 h under Ar atmosphere. The electrolyte used was 1 M NaPF₆ in ethylene carbonate and dimethyl carbonate mixture (EC:DMC), in 1:1 vol ratio, with water content < 50 ppm (measured by Karl Fischer titration using Sigma Aldrich titration reagent). Swagelok cells were assembled in an argon filled glovebox with oxygen and water levels below 1 ppm. The mix of pristine or treated NaVO₂ active material and acetylene black was used as the working electrode, and Na metal as both counter and reference electrodes with two glass fiber (GF/B, 200 μm thick) separators between working and counter electrodes. Galvanostatic charge and discharge cycles were conducted at room temperature with different C rates in voltage window between 1.2 and 3.8 V, starting cycling from the oxidation for both treated and pristine powders.

XPS measurements were recorded using XPS K alpha spectrometer equipped with monochromated 450 W Al K_α source. The pressure of the system was below 10⁻⁷ Pa. The sample was previously dried at 120 °C under Ar atmosphere for 12 h in order to remove surface contaminations. The EDS measurements were performed using TEAM™ EDS System for the SEM with Apollo X Silicon Drift Detector (SDD) with 15 kV voltage.

3. Results and discussion

Fig. 1 shows a schematic representation of the liquid exfoliation process of synthesized NaVO₂ powders. The process was achieved in water, owing to the high sensitivity of NaVO₂ to moisture. In the case of Na removal from the NaVO₂, water plays role of the oxidizer. During this process, the spontaneous oxidation of NaVO₂ by water leads to the formation of (partially) desodiated Na_xVO₂ phase (reaction 1).



Important differences were observed during the NaVO₂ delamination process between the suspension at the beginning and at the end of the experiment. During initial stages, NaVO₂ powder quickly precipitated after removing from sonication, while after a few filtration redispersion steps, decrease of ionic strength of the dispersions yields uniform dark colloidal suspensions for a couple of hours. Those observations may evidence the achievement of the small and well dispersed particles. About 40 wt% of the initial powder was recovered after treatment. This could be partially due to Na ion removal though it does not explain such big losses and a partial dissolution of the smallest NaVO₂ particles is assumed to occur during the process.

SEM images (Fig. 2b,c) do not show complete delamination of the NaVO₂, that is total separation of the vanadium oxide layers. However, treated NaVO₂ powders are composed of numerous thin sheets stacked into flakes, together with some noticeable two dimensional flakes as observed for other materials such as MXene prepared from etching in acid electrolytes [18]. Such a morphology supports the partial

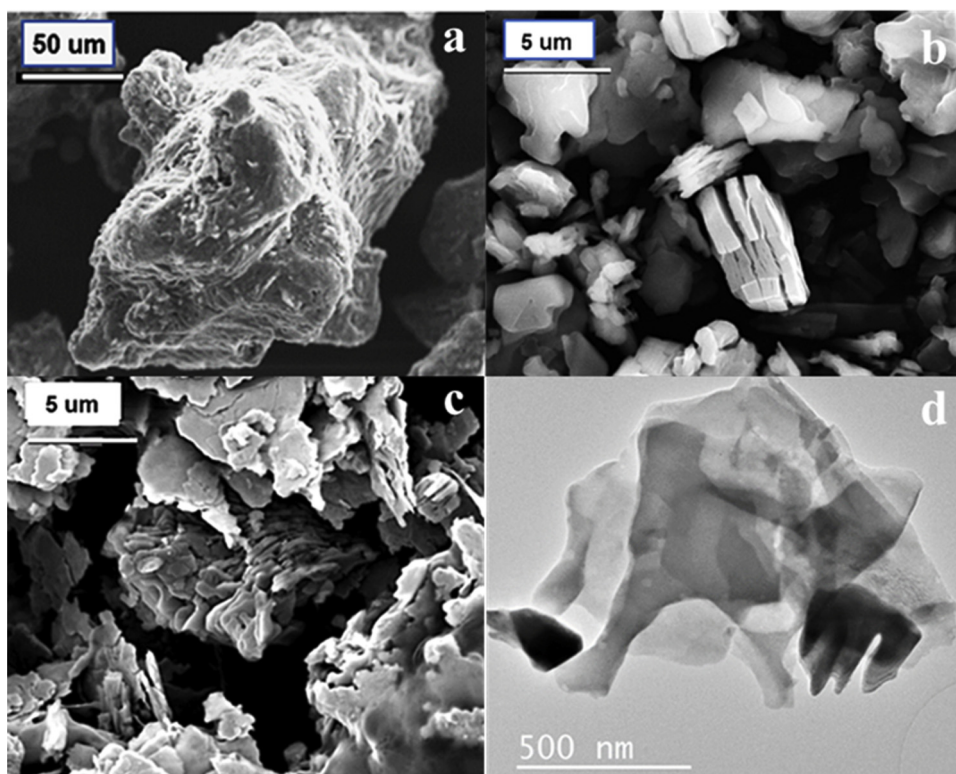


Fig. 2. SEM images of the NaVO₂ powders: a) pristine O3 - type, b) treated and freeze – dried c) treated and heated to 200 °C under Ar, d) TEM image of NaVO₂ treated and heated to 200 °C under Ar.

delamination of the layered compound, which is also in a good agreement with weight loss of powder measured during delamination, as mentioned above. The difference between treated freeze dried sample and treated heated one mainly lies on the flake shape. In the case of the freeze dried powder, well organized stacks of parallel sheets together with 2D like shaped layers are visible. Although the flake like structure remains similar for both samples, the flakes in case of heated sample look more disordered.

The diameter of the treated NaVO₂ flakes is beyond 1 μm, but are composed with nanosheets, as shown on the TEM image (Fig. 2d). In addition, SEM images show relatively smoothed edges of the flakes, which supports the existence of partial dissolution of smallest particles of NaVO₂ in water.

The XRD pattern of pristine NaVO₂ (Fig. 3, red color) shows a mixture of O3 NaVO₂ and P2 Na_{0.7}VO₂. This is consistent with previous results showing the high sensitivity of stoichiometric O3 NaVO₂ which easily converts to Na deficient P2 Na_{0.7}VO₂ when exposed to air even for a short time [24]. Aside from the peaks corresponding to O3 and P2 structures, there are few peaks corresponding to V₂O₃, which result from the reduction of remaining V₂O₅ in the NaVO₃ starting material. The comparison of the XRD pattern of pristine sample to the treated NaVO₂ powders ones (Fig. 3, blue and green colors) shows the loss of all Bragg peaks attributed to P2 and O3 Na_xVO₂ layered materials. The remaining diffraction peaks with small intensity can all be attributed to unreacted V₂O₃ impurities. Those observations result in the conclusion that both treated powders lost long range periodicity, in accordance with TEM observations showing transparent nanosheets, which makes difficult the identification of the structural changes of the treated samples. Moreover, freeze dried and dried by heating under Ar samples display almost identical patterns, except one key feature which lies on the presence of a peak at low angle for the freeze dried powder. This peak corresponds to (001) plane of a 2D structure with an interlayer distance around 7 Å larger than that (ca 5.5 Å) of pristine NaVO₂. This can be the evidence of the successful replacement of Na by water, which

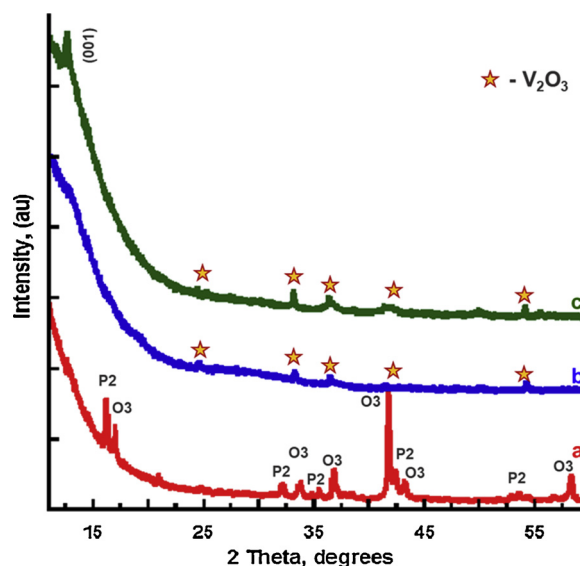


Fig. 3. XRD pattern of the a) pristine NaVO₂ (red) and b) treated and Ar-dried NaVO₂ to 200 °C (blue) c) treated, freeze – dried NaVO₂ (green), the identified peaks correspond to V₂O₃ impurities.

even after freeze drying process, pillar the layers. In contrast, by drying the sample at 200 °C under Ar atmosphere, the interlayer water was removed without long range restacking as confirmed by the absence of diffraction peaks. This assumption is also fully consistent with the SEM images of the freeze dried sample, which shows more layered like structure compare to more separated sheets of Ar dried treated NaVO₂.

The XPS analysis of the pristine O3 NaVO₂ shows peaks corresponding mainly to Na(1 s), O (1S) and C(1 s) levels indicating the presence of NaOH and/or Na₂CO₃ on the surface with a thickness high enough to prevent the detection of V(2p) peaks in agreement with the

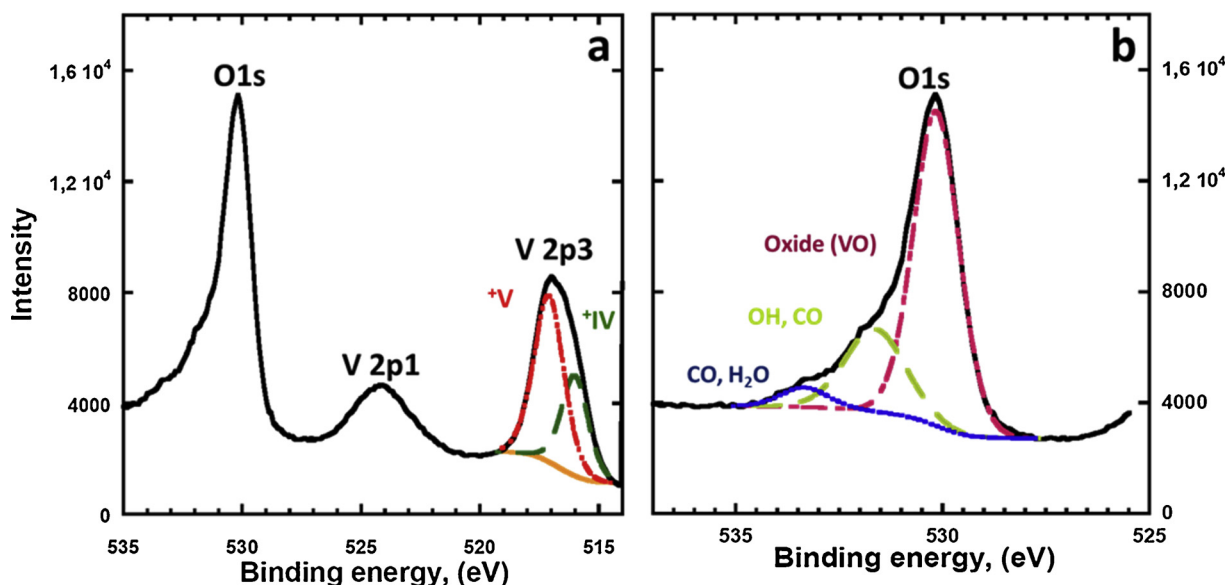


Fig. 4. XPS analysis of treated NaVO_2 heated to $200\text{ }^\circ\text{C}$ under Ar: a) fitting of the V2p3 peak, b) fitting of the O1s peak.

Table 1
Reported XPS data.

Material	V2p3	FWHM (eV)	$\Delta_{\text{O1s}/\text{V2p3/2}}$ (eV)
	BE (eV)		
V2O5	517,0 [30]	1,4	12,8
	517,7 [31]	0,9	12,8
VO2	515,65 [30]	4,0	14,35
	516,2 [31]	3,2	13,7
V2O3	515,2 [30]	4,8	14,84
	515,9 [31]	4,9	14,4

well known high air sensitivity of O3 NaVO_2 . Differently, V, O and C were identified in the treated NaVO_2 samples. V2p and O1s peaks were fitted using Lorentz-Gaussian type curves (Fig. 4a). It can be seen from Table 1 that there is a large spread on the reported values, especially for the V^{4+} and V^{3+} oxidation states. The integration of the peaks of the V2p3/2 and V2p1/2 levels leads to a consistent ratio of 2:1 which is generally found when fitting the V2p energy level XPS signals [29]. Different methods have been proposed in the literature to calculate the oxidation states of vanadium and their relative (atomic) content from the fitting of the V2p peaks. Several authors only use the V2p3/2 signal for data analysis [30–33], while others also take the V2p1/2 signal into account for subtracting the background [34]. In our case because of the proximity of O1s and the V2p1/2 peaks affects the background determination accuracy, only V2p3 was considered for fitting in agreement with reported data [30,31]. Also, Mendialdua et al. [30] have shown that the difference in binding energy ($\Delta_{\text{O1s}/\text{V2p3/2}}$) between the O1s and V2p3/2 level should be taken into account to accurate determination of the V oxidation state. The fitting of V2p3/2 peak reveals two different contributions at 517.09 and 516 eV, in agreement with the broad and asymmetric peak shape, corresponding to V^{+V} and V^{+IV} oxidation states, respectively [30,31]. The intensity of the peak at 517.09 eV (V^{+V}) was notably higher than the one at 516 eV (V^{+IV}) (Fig. 4a). The $\Delta_{\text{O1s}/\text{V2p3/2}}$ is around 13 and 14 eV for V^{+V} and V^{+IV} , respectively, which well agrees with the literature [30,31]. Table 2 lists the results of the fitting, as well as the relative atomic content. No V^{+III} signal was detected during this XPS analysis showing that the surface is free of V_2O_3 , differently from the bulk as revealed by XRD experiment. The fitting of the O1s peak (Fig. 4b) shows a peak at 530.15 eV corresponding to O1s in VO_x [30], together with the contributions from the contamination surface layer, which can be water (peaks at 531.6

Table 2
Fitted XPS data.

Name	Peak BE (eV)	FWHM (eV)	Atomic %
C1s CC, CH	284.55	1.42	30.96
C1s C O	286.22	1.44	4.67
C1s COO/C=O	288.62	1.44	3.40
O1s A (VOx)	530.1	1.30	32.18
V2p3/2 (IV)	516.00	1.32	4.98
V2p3/2 (V)	517.09	1.47	9.23
Na1s	1071.56	1.41	1.36
V2p3/2 (III)	515.18	1.34	0.00
O1s B (OH, CO)	531.63	1.71	11.16
O1s C (CO, H2O)	533.34	1.32	2.05

and 533.4 eV). Another important feature is the peak at 1071.5 eV, which corresponds to Na (1s). The low intensity of the signal indicates a small amount of Na^+ in the compound. The atomic ratio, which were calculated from the fitting of the peaks, gives a composition of roughly $\text{Na}_{0.8}\text{V}_{0.8}^{+IV}\text{V}_{1.2}^{+V}\text{O}_5$ or $\text{Na}_{0.8}\text{V}_2\text{O}_5$ for the surface of the treated NaVO_2 sample. It confirms a partial removal of Na ions from the structure, but reveals that this removal comes with an oxidation of the V^{+III} into both V^{+IV} and V^{+V} at least on the material surface.

The EDS analyses show presence of Na, V and O peaks (See Fig. 5). Taking into account estimated composition of the sample (Table 3), the average composition of the powder is $\text{Na}_{0.16}\text{V}_3\text{O}_5$. This results in an average oxidation state of the vanadium of ($\text{V}^{+3.3}$) in the bulk powder. This finding is first consistent with partial sodium removal from the original NaVO_2 structure. Also, the comparison of the EDS and the XPS analyses shows that the oxidation state of vanadium on the surface of the material differs from the one in the bulk, consistent with a higher reactivity of the surface versus the bulk.

Both treated samples were electrochemically tested in the 1.2–3 V vs Na voltage range. However freeze dried NaVO_2 exhibited poor capacity and cycling life. Such performance could be attributed to presence of water in between the VO_2 layers which is known to be detrimental to electrochemical performance [35]. Then only the sample dried at $200\text{ }^\circ\text{C}$ has been further investigated. Fig. 6 shows the electrochemical galvanostatic charge/discharge characterizations of the treated (red) and pristine (black color) NaVO_2 in the 1.2–3 V vs Na voltage range. The electrochemical signature of the synthesized pristine NaVO_2 was similar to the previously reported ones for O3 type phase [28], which well agrees with the XRD data. More specifically, the presence of

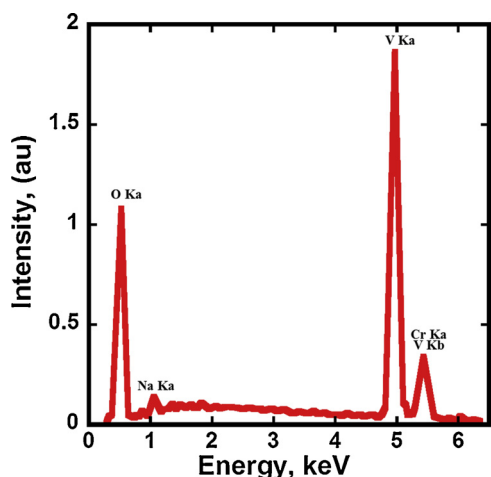


Fig. 5. EDS analysis of the treated NaVO₂ sample.

Table 3

Estimated chemical composition of the treated NaVO₂ sample from EDS analysis.

Element	Wt %	At %
C K	00.04	00.11
O K	33.01	60.38
NaK	01.44	01.83
AlK	00.48	00.52
SiK	00.47	00.49
PtM	01.18	00.18
S K	00.29	00.26
V K	62.78	36.06
CrK	00.31	00.17

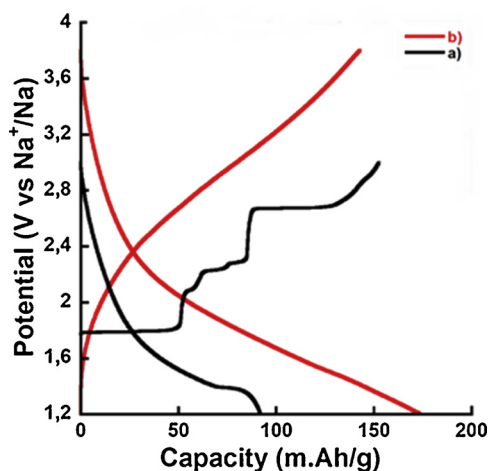


Fig. 6. GCPL curves of the a) pristine NaVO₂ (black) and b) water treated and heated to 200 °C under Ar (red).

several potential plateaus on charge (oxidation) evidences Na ion de intercalation process through multiple two phase transformations in the 1.2–3 V vs Na potential range. The discharge (reduction) cycle shows a drastic decrease of the capacity, in good agreement with the results reported by Didier et al. [28]. Indeed, the removal of Na ions from the structure by potential excursion up to 2.8 V is fully reversible [24] while beyond 3 V an irreversible crystallographic phase transformation occurs leading during the first discharge and the second charge to a small capacity and poor electrochemical signature [28].

Drastic changes were observed in the electrochemical signatures of treated and dried NaVO₂ samples (Fig. 6, red color). First, the open

circuit voltage (OCV) of the treated NaVO₂ sample (3.1 V), is almost 1.5 V higher than the one measured for pristine O3 NaVO₂. This is in accordance with the XPS results, which spotted the formation of V^{+IV}/V^{+V} from pristine sample. Second, treated sample shows nearly linear potential slopping discharge voltage profile and none of the multi step reaction potential plateaus observed for pristine sample are present. These points out a major change in the electrochemical behavior, moving from 2 phase reaction process to a one phase like process. Another difference is the significant enlargement of the operating potential window, from 1.2 V to 3.8 vs. Na/Na⁺ compared to pure O3 NaVO₂ with potential window from 1,2 to 2,5 V. Such large voltage window could suggest that several oxidation states (V⁺⁵ to V⁺⁴ and V⁺³) are involved. This suggestion is consistent with the XPS and EDS analyses. Moreover, treated NaVO₂ can achieve capacity as high as 160 mA h g⁻¹ at C/10 that is about twice larger than that of the pristine sample in the same potential range as well as 120 mA h/g at C/5 rate together with 90% coulombic efficiency. These results show that the modification of the long range ordering of NaVO₂ by even partial exfoliation results in drastic change of the electrochemical signature. Another interesting effect of the partial exfoliation of NaVO₂ is the suppression of irreversible structure changes. This allows operating compounds in a larger voltage range thus making accessible several redox couples leading to a drastic increase of the reversible capacity. Extending this concept involving partial disordering in the stacking sequence to other layered compounds could pave the way for the design of new materials with larger accessible voltage range and tuned electrochemical properties allowing enlarging reversible capacity.

4. Conclusions

In summary, the work presented here shows that a careful modification of the structure of NaVO₂ by a simple liquid exfoliation process in water can lead to drastic change in the electrochemical performance for energy storage applications. XRD and electrochemical cycling techniques show that we managed to change the long range order of the layered materials. While we do not achieve reaching full delamination, this has allowed suppressing irreversible structure changes known to restrict reversible capacity. The galvanostatic cycling of the treated and Ar dried powder showed close to linear voltage profile together with enlarged voltage window leading to the possible activation of several redox couple and a drastic increase of the accessible reversible capacity. Although additional work has to be done to improve the high rate performance via a careful selection of intrinsic properties of layers, these results open the way to explore randomly stacked layered material with enlarged operating voltage windows and high reversible capacity.

Acknowledgements

Authors would like to thank the Agence Nationale de la Recherche (LABEX Storex program) for funding.

References

- [1] P. Simon, Y. Gogotsi, Materials for electrochemical capacitors, *Nat. Mater.* 7 (2008) 845–854, <https://doi.org/10.1038/nmat2297>.
- [2] B.E. Conway, *Electrochemical Supercapacitors: Scientific Fundamentals and Technological Applications*, Springer US, Boston, MA, 1999.
- [3] V. Augustyn, P. Simon, B. Dunn, Pseudocapacitive oxide materials for high-rate electrochemical energy storage, *Energy Environ. Sci.* 7 (2014) 1597, <https://doi.org/10.1039/c3ee44164d>.
- [4] N.-L. Wu, Nanocrystalline oxide supercapacitors, *Mater. Chem. Phys.* 75 (2002) 6–11, [https://doi.org/10.1016/S0254-0584\(02\)00022-6](https://doi.org/10.1016/S0254-0584(02)00022-6).
- [5] T. Brousse, M. Toupin, R. Dugas, et al., Crystalline MnO[sub 2] as possible alternatives to amorphous compounds in electrochemical supercapacitors, *J. Electrochem. Soc.* 153 (2006) A2171, <https://doi.org/10.1149/1.2352197>.
- [6] T. Brousse, P.-L. Taberna, O. Crosnier, et al., Long-term cycling behavior of asymmetric activated carbon/MnO₂ aqueous electrochemical supercapacitor, *J. Power Sources* 173 (2007) 633–641, <https://doi.org/10.1016/j.jpowsour.2007.04.074>.

- [7] F. Béguin, E. Frackowiak, *Supercapacitors: Materials, Systems, and Applications*, Wiley-VCH, Weinheim, 2013.
- [8] M. Acerce, D. Voiry, M. Chhowalla, Metallic 1T phase MoS₂ nanosheets as supercapacitor electrode materials, *Nat. Nanotechnol.* 10 (2015) 313–318, <https://doi.org/10.1038/nnano.2015.40>.
- [9] V. Nicolosi, M. Chhowalla, M.G. Kanatzidis, et al., Liquid exfoliation of layered materials, *Science* 340 (2013), <https://doi.org/10.1126/science.1226419> 1226419–1226419.
- [10] R. Ruoff, Calling all chemists: graphene, *Nat. Nanotechnol.* 3 (2008) 10–11, <https://doi.org/10.1038/nnano.2007.432>.
- [11] M. Osada, T. Sasaki, Exfoliated oxide nanosheets: new solution to nanoelectronics, *J. Mater. Chem.* 19 (2009) 2503, <https://doi.org/10.1039/b820160a>.
- [12] A.B. Bourlinos, V. Georgakilas, R. Zboril, et al., Liquid-phase exfoliation of graphite towards solubilized graphenes, *Small* 5 (2009) 1841–1845, <https://doi.org/10.1002/sml.200900242>.
- [13] K.S. Novoselov, V.I. Fal'ko, L. Colombo, et al., A roadmap for graphene, *Nature* 490 (2012) 192–200, <https://doi.org/10.1038/nature11458>.
- [14] D.R. Dreyer, S. Park, C.W. Bielawski, R.S. Ruoff, The chemistry of graphene oxide, *Chem. Soc. Rev.* 39 (2010) 228–240, <https://doi.org/10.1039/B917103G>.
- [15] J.N. Coleman, Liquid exfoliation of defect-free graphene, *Acc. Chem. Res.* 46 (2013) 14–22, <https://doi.org/10.1021/ar300009f>.
- [16] J.N. Coleman, M. Lotya, A. O'Neill, et al., Two-dimensional nanosheets produced by liquid exfoliation of layered materials, *Science* 331 (2011) 568–571, <https://doi.org/10.1126/science.1194975>.
- [17] Q.H. Wang, K. Kalantar-Zadeh, A. Kis, et al., Electronics and optoelectronics of two-dimensional transition metal dichalcogenides, *Nat. Nanotechnol.* 7 (2012) 699–712, <https://doi.org/10.1038/nnano.2012.193>.
- [18] B. Anasori, M.R. Lukatskaya, Y. Gogotsi, 2D metal carbides and nitrides (MXenes) for energy storage, *Nat. Rev. Mater.* 2 (2017), <https://doi.org/10.1038/natrevmats.2016.98>.
- [19] Y. Dall'Agnese, P.-L. Taberna, Y. Gogotsi, P. Simon, Two-dimensional vanadium carbide (MXene) as positive electrode for sodium-ion capacitors, *J. Phys. Chem. Lett.* 6 (2015) 2305–2309, <https://doi.org/10.1021/acs.jpcllett.5b00868>.
- [20] Y. Dall'Agnese, P. Rozier, P.-L. Taberna, et al., Capacitance of two-dimensional titanium carbide (MXene) and MXene/carbon nanotube composites in organic electrolytes, *J. Power Sources* 306 (2016) 510–515, <https://doi.org/10.1016/j.jpowsour.2015.12.036>.
- [21] M.G. Barker, A.J. Hooper, Reactions of sodium oxide with the oxides VO₂, V₂O₃, VO, and vanadium metal, *J. Chem. Soc. Dalton Trans.* 1517 (1973), <https://doi.org/10.1039/dt9730001517>.
- [22] B.L. Chamberland, S.K. Porter, A study on the preparation and physical property determination of NaVO₂, *J. Solid State Chem.* 73 (1988) 398–404, [https://doi.org/10.1016/0022-4596\(88\)90124-7](https://doi.org/10.1016/0022-4596(88)90124-7).
- [23] M. Onoda, Geometrically frustrated triangular lattice system Na_xVO₂: superparamagnetism in $x = 1$ and trimerization in $x \approx 0.7$, *J. Phys. Condens. Matter* 20 (2008) 145205, <https://doi.org/10.1088/0953-8984/20/14/145205>.
- [24] D. Hamani, M. Ati, J.-M. Tarascon, P. Rozier, Na_xVO₂ as possible electrode for Na-ion batteries, *Electrochem. Commun.* 13 (2011) 938–941, <https://doi.org/10.1016/j.elecom.2011.06.005>.
- [25] C. Didier, M. Guignard, J. Darriet, C. Delmas, O³⁻-Na_xVO₂ system: a superstructure for Na_{1/2}VO₂, *Inorg. Chem.* 51 (2012) 11007–11016, <https://doi.org/10.1021/ic301505e>.
- [26] O. Szajwaj, E. Gaudin, F. Weill, et al., Investigation of the new P³⁻-Na_{0.60}VO₂ phase: structural and physical properties, *Inorg. Chem.* 48 (2009) 9147–9154, <https://doi.org/10.1021/ic9008653>.
- [27] M. Guignard, C. Didier, J. Darriet, et al., P₂-Na_xVO₂ system as electrodes for batteries and electron-correlated materials, *Nat. Mater.* 12 (2013) 74–80, <https://doi.org/10.1038/nmat3478>.
- [28] C. Didier, M. Guignard, C. Denage, et al., Electrochemical Na-deintercalation from NaVO₂, *Electrochem. Solid-State Lett.* 14 (2011) A75, <https://doi.org/10.1149/1.3555102>.
- [29] M.C. Biesinger, L.W.M. Lau, A.R. Gerson, R.S.C. Smart, Resolving surface chemical states in XPS analysis of first row transition metals, oxides and hydroxides: Sc, Ti, V, Cu and Zn, *Appl. Surf. Sci.* 257 (2010) 887–898, <https://doi.org/10.1016/j.apsusc.2010.07.086>.
- [30] J. Mendialdua, R. Casanova, Y. Barbaux, XPS studies of V₂O₅, V₆O₁₃, VO₂ and V₂O₃, *J. Electron. Spectrosc. Relat. Phenom.* 71 (1995) 249–261, [https://doi.org/10.1016/0368-2048\(94\)02291-7](https://doi.org/10.1016/0368-2048(94)02291-7).
- [31] G. Silversmit, D. Depla, H. Poelman, et al., Determination of the V2p XPS binding energies for different vanadium oxidation states (V⁵⁺ to V⁰⁺), *J. Electron. Spectrosc. Relat. Phenom.* 135 (2004) 167–175, <https://doi.org/10.1016/j.elspec.2004.03.004>.
- [32] J.S. Bonso, A. Rahy, S.D. Perera, et al., Exfoliated graphite nanoplatelets-V₂O₅ nanotube composite electrodes for supercapacitors, *J. Power Sources* 203 (2012) 227–232, <https://doi.org/10.1016/j.jpowsour.2011.09.084>.
- [33] Y. Liu, M. Clark, Q. Zhang, et al., V₂O₅ nano-electrodes with high power and energy densities for thin film Li-ion batteries, *Adv. Energy Mater.* 1 (2011) 194–202, <https://doi.org/10.1002/aenm.201000037>.
- [34] D. Choi, G.E. Blomgren, P.N. Kumta, Fast and reversible surface redox reaction in nanocrystalline vanadium nitride supercapacitors, *Adv. Mater.* 18 (2006) 1178–1182, <https://doi.org/10.1002/adma.200502471>.
- [35] C.-Y. Lee, A.C. Marschlok, A. Subramanian, et al., Synthesis and characterization of sodium vanadium oxide gels: the effects of water (n) and sodium (x) content on the electrochemistry of Na_xV₂O₅·nH₂O, *Phys. Chem. Chem. Phys.* 13 (2011) 18047, <https://doi.org/10.1039/c1cp21658a>.